Monitoring the Luminosity Spectrum*

M.N.Frary and D.J.Miller
Department of Physics and Astronomy,
University College London,
Gower St., London W.C.1E. 6BT, U.K.

November 6, 1991

Abstract

Beamstrahlung at a high energy linear collider will give a long tail to the distribution of effective collision energy. There will also be a significant momentum spread within each accelerated bunch. We discuss ways of monitoring these effects, with special attention to studies of the possible structures at the top-antitop threshold, and conclude that sufficiently precise techniques can be devised - if the momentum spread in the linac can be kept small.

1 Statement of the Problem.

In all energy regions at a high energy linear collider it will be necessary to calculate a luminosity spectrum $\mathrm{d}\mathcal{L}/\mathrm{d}\sqrt{s}$ for each running period which must be unfolded from the rates for the observed signal-channels to give cross sections as a function of energy. The requirements will be most stringent close to a narrow structure such as the top-antitop threshold enhancement [1]. If the top-antitop threshold were at $\sqrt{s} = 250GeV$ a resolution in $\sqrt{s}$ of about $\pm 250MeV$ (1 part in 1000) would be needed fully to resolve the details of the 'toponium remnant' peak. Any worsening of the resolution from this level reduces sensitivity to the physics (see main report from top-antitop working- group, in these proceedings).

The monitoring must have two parts:

*Prepared for the Working Groups on Linear Collider Physics, DESY, Hamburg, 2/3 September 1991; with added material presented at the Workshop on Physics and Experiments with Linear Colliders, Saariselka, Finland 9-12 September 1991

a) Determining the absolute momenta and the momentum spread of the beams. Groups working at SLC are already doing this with special spectrometers to look at the beam bunches after they have passed the collision point. Their claimed precision of around $\pm 20 MeV$ in 50 GeV [3], (1 part in 2500) will be adequate if it can be maintained at higher energy. We review their work briefly in Section 2 below.

b) Measuring the actual effective luminosity of the colliding beams, including the effects of misalignment and beamstrahlung. Our favoured technique for doing this is to monitor the acollinearity of Bhabha scattering events, as described in Section 3 below. This is the only process which will have the accuracy required for toponium threshold studies, and it has much larger statistics than any other channel. Other final states such as W^+W^- and $Z^0\gamma$ may be useful away from narrow structures. They are discussed briefly in Section 4.

The situation at a linear collider is very different from LEP where the beams have a well defined collision energy and it has been sufficient to calculate one integrated luminosity for each energy-setting of the machine. Bhabha-scattering in the region from 40 to 120 milliradians at LEP gives a comparable statistical sample to the sample of hadronic Z^0 decays at resonance, and systematic errors on the absolute luminosity measurement have been reduced to significantly less than 1%, e.g. [2]. There is no reason to believe that the absolute normalisation of the luminosity spectrum at a linear collider cannot be measured to the same kind of precision using Bhabha scattering.

But the finite beamspread ($\simeq$ 50 MeV) at LEP will soon become a significant limitation on the Z^0 lineshape fit. The systematic errors from the absolute beam energy measurement are being reduced by depolarisation techniques, and by better understanding of the flux-loops used for secondary calibration. New methods are being devised to reduce the errors on the overall normalisation, and much larger statistics will be available over the next two years. It will then be desirable to measure luminosity spectra at LEP using the techniques described in Section 3; but only if the tracking detectors have adequate resolution in θ. There could be difficulties due to correlated dispersion in the two circulating beams [5]. If lower energy electrons in LEP preferentially meet lower energy positrons, and higher energy electrons meet higher energy positrons, then the distributions of Δp and θ_A (as described below) will not be such a good guide to the desired distribution of $\sqrt{s}$. Beamstrahlung will remain insignificant at the relatively low

luminosity required for Z^0 studies.

2 Precise measurement of beam energy

Work is now going on at the Stanford final focus test facility and at the SLC to develop techniques for monitoring the beam properties. Kent *et al* [3] make three successive bends in the extraction-line beams of SLC, after the intersection point (Figure 1). The first and third are horizontal bends,

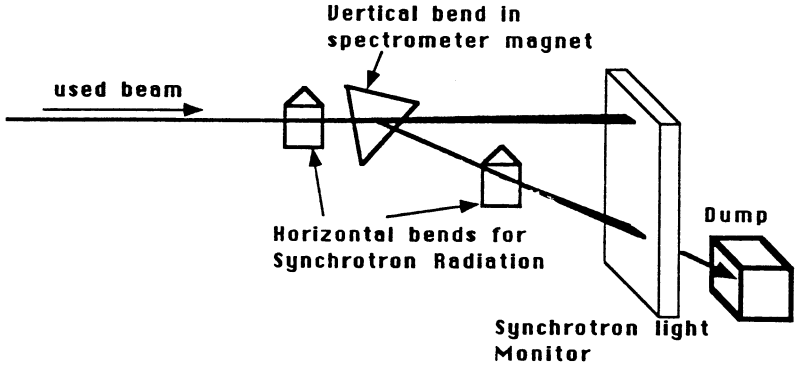

Figure 1: Principle of the SLC extraction- line spectrometer [3] - with the bend-angles greatly exaggerated.

producing horizontal 'swaths' of synchrotron radiation. The intermediate vertical bend in a precision spectrometer magnet separates these two swaths so that their relative positions can be monitored by a single detector. They claim a precision on the absolute beam energy of better than 1 part in 2000. There appears to be no reason why this technique, or equivalent techniques with faster readout to allow for different bunch structures, should not be usable at a higher energy machine. It will be necessary to monitor both the absolute energy and the momentum spread in each beam.

Of course 'used beam' will already be distorted by beamstrahlung, if the bunches have collided, and it will be necessary regularly to separate the beams to make clean measurements of the momentum and its spread. Techniques also exist at SLAC to monitor the flux of beamstrahlung photons on a bunch by bunch basis. But no amount of careful measurement on the used beam can measure the effect of beamstrahlung and momentum spread on the luminosity spectrum for high energy collisions. This must be

extracted from analysis of a suitable sample of collision events, as discussed in the next two sections.

3 Bhabha scattering

3.1 Use of acollinearity.

It is impossible directly to monitor the luminosity spectrum $d\mathcal{L}/d\sqrt{s}$ with the precision on $\sqrt{s}$ required for top-antitop threshold studies because no detector can measure final state energies to 1 part in 1000. But the distribution of the longitudinal momentum mismatch $\Delta p = p_+ - p_-$ is very closely related to the distribution of $\sqrt{s} = 2\sqrt{p_+ p_-}$. The acollinearity angle θ_A of Bhabha-scattering events is a direct measure of Δp at the moment of collision ($\theta_A = \pi - \theta_+ - \theta_-$ for the scattered particles). For small θ_A and low radiated energy loss, $\theta_A \simeq \frac{\Delta p}{p_b} \sin\theta$, where $\theta \simeq \theta_+ \simeq \theta_-$.

There are three distinct causes of momentum mismatch which we have investigated in a Monte Carlo study:

a) Initial state radiation. This is inescapable, and is the same for all accelerator designs. Studies with the BABAMC generator [4] show that there is always a clear spike of events with very small radiative energy loss, see Figure 3.

b) Beamstrahlung, the scattering of incoming electrons and positrons from the electromagnetic field concentration of the opposing beam bunch. This again produces a clear spike of events with small energy losses and long tails of events with large losses, see Figure 2 . The amount of beamstrahlung varies considerably between different linac designs. This has been studied with the SLAC BEAMSPEC program (written by T.Barklow, set up for us by W.Kozanecki). The beam-designs, see Table 1, were the similar to those used in the study of the top-antitop excitation curve, as reported in the section of the main working group report on the Threshold Energy Scan (W.Kozanecki comments that the linac parameters were optimised for 250 GeV on 250 GeV and may overestimate beamstrahlung effects at a supposed top-antitop threshold of around 125 GeV on 125 GeV). Linac designs with very high luminosity, such as 'Palmer G' have such large momentum spread and severe beamstrahlung that there could be no possibility of using them for top-antitop threshold studies.

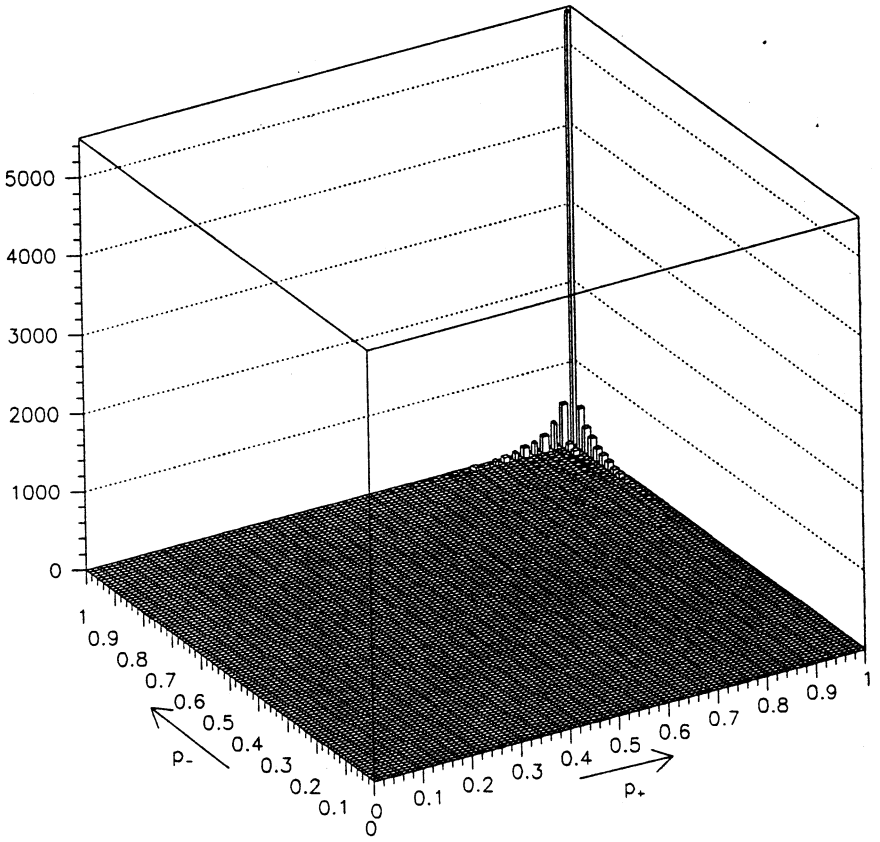

Figure 2: LEGO plot of the two individual beam momenta p_+ and p_-, normalised to the nominal momentum p_{nom}, after beamstrahlung, for Beam 1 [6].

c) Momentum spread in the linac beams. This also varies widely between designs. We have taken account of it by sampling from a gaussian distribution. See Table 1 for the r.m.s. spreads assumed for each beam.

The measured acollinearity distribution for a given accelerator setting will contain information on the combined effects of these three causes of missmatch in a way which closely represents their effect on a signal channel. Measurement errors on the acollinearity angle are discussed in Subsection 3.2 below.

If the sources of fluctuations in $\sqrt{s}$ were all small and gaussian then the relation between the spread in $\sqrt{s}$, the spread in Δp, the spread in the

Table 1: Properties assumed for various linac designs.

Parameter	Beam 1[6]	Beam 2[7]	Beam 3[8]
Luminosity ($10^{33} cm^{-2} s^{-1}$)	1.4	4.4	2.1
Fraction of events with $\Delta p < 0.01 E_b$ from Beamstrahlung.	0.45	0.26	0.54
Spread in E_b %.	0.17	0.57	0.1

acollinearity angle and the spread in the beam momentum would be simply

$$\sigma_{\sqrt{s}} = \sigma_{\Delta p} = \sigma_{\theta_A} \frac{p_b}{\sin\theta} = \sqrt{2}\sigma_{p_b} \tag{1}$$

Figure 3 shows distributions of the acollinearity angle θ_A in three differ-

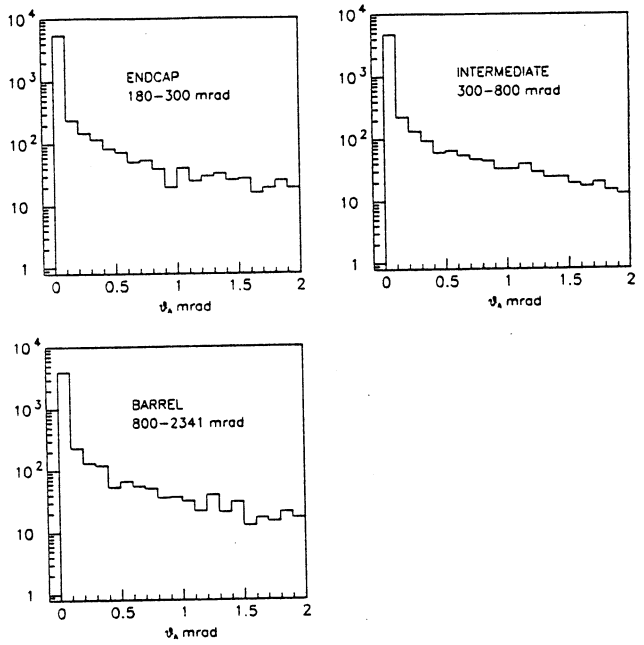

Figure 3: Effect of initial state radiation on the acollinearity angle θ_A for Bhabha scattering in three different angular ranges

ent ranges of the Bhabha scattering angle θ for events taken directly directly from the BABAMC generator. There are 54% of the events in the spike with

$\theta_A <$ 0.1 mrad. in the endcap region, 48% in the intermediate region and 40% in the barrel region. From equation (1) this corresponds approximately to values for $\sigma_{\sqrt{s}}/\sqrt{s}$ of 1 part in 4000, 1 part in 10^4 and 1 part in $1.7\,10^4$, respectively. The precision is better in the barrel region because of the $\sin\theta$ factor in equation (1), but the rate is much lower (see Table 3). The effects of initial state radiation alone do not destroy the possibility of observing very sharp features in the luminosity spectrum.

What happens when we add first beamstrahlung and then a finite momentum spread can be seen in Figure 4 for Beam 1 [6], with Bhabha scat-

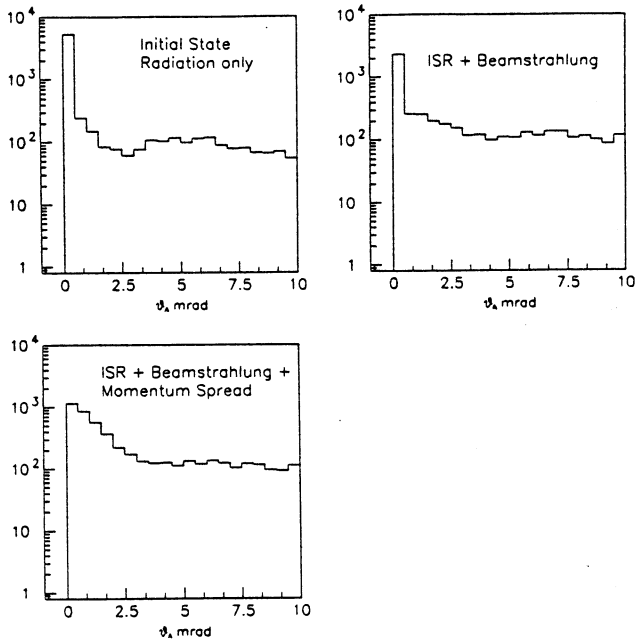

Figure 4: Effect of Beamstrahlung and beam-momentum-spread on the acollinearity distribution with Beam 1 [6] in the intermediate range of Bhabha scattering angles $300 < \theta < 800$ milliradians.

tering in the intermediate range of angles. Table 2 summarises how the number of events in the spike with $\theta_A < 1$ milliradian changes, for all three of the good linac designs. Beam 2 would clearly be unsuitable for top-antitop threshold studies if it had the assumed amount of momentum spread. The other two beams do still have a distinct spike of events close to the nominal momentum, so it should be possible both to resolve some of the sharpness of the threshold step (as confirmed by Miquel and Orteu), and to measure

Table 2: Fraction of events with $\theta_A < 1$ mrad. $300 < \theta < 800 mrad.$

	Beam 1[6]	Beam 2[7]	Beam 3[8]
Initial state radiation.	0.56	0.56	0.56
ISR + Beamstrahlung.	0.24	0.13	0.25
ISR + Beamstrahlung + beam spread.	0.18	0.05	0.22

the corresponding luminosity spectrum using Bhabha scattering.

3.2 Measurement of acollinearity

The acollinearity angle θ_A can be measured accurately if the detector has good resolution in the beam direction, or radially in the endcap region, for at least two well spaced points on every track. A silicon detector with transverse strips would give adequate resolution, $\pm$ 0.05 mm.(say), for the first point. The second point could come from a drift chamber - either outside the barrel tracking-detector or against the face of the electromagnetic endcap detector, depending on the scattering angle of the Bhabhas used. If each track is measured with an r.m.s. error $\sigma_\theta = \sigma_{\theta_A}/\sqrt{2}$ then, from equation (1), $\sigma_{\sqrt{s}}/\sqrt{s} = \sigma_\theta/\sqrt{2}\sin\theta$. For a precision of 1 part in 1000 on $\sqrt{s}$ the tracks would need to be measured with $\sigma_\theta = 0.25$ milliradians for scattering close to the expected forward cutoff at 180 milliradians, with $\sigma_\theta = 1.1$ milliradian in the intermediate angular region, or with $\sigma_\theta = 1.7$ milliradians for equatorial scattering. With the second detector 1 metre away from the first, this would require a positional accuracy of 0.25 millimetres in radius for an endcap drift chamber at 180 milliradians; or 1.7 millimetres along the beam direction for a 'z-chamber' in the barrel region. These are reasonable requirements, but sufficiently precise that the detectors will have to be carefully built and carefully surveyed.

3.3 Fitting strategies

Some simplifying assumptions are presented to clarify the relation between the distributions of θ_A and $\sqrt{s}$. On the basis of this understanding it is possible to outline the fitting procedures which will be needed to determine the luminosity spectrum as a function of $\sqrt{s}$.

3.3.1 Simplified model

Neglecting beamspread, we assume that the effect of beamstrahlung and initial state radiation on each interacting beam is to produce a tail towards low momenta, with a peak at the nominal beam momentum p_{nom}. Introducing the variables

$$x_+ = 1 - \frac{p_+}{p_{nom}} \text{ and } x_- = 1 - \frac{p_-}{p_{nom}}. \quad (2)$$

$$x_s = 1 - \frac{\sqrt{s}}{2p_{nom}} = 1 - \sqrt{(1-x_+)(1-x_-)}$$

$$\simeq \frac{(x_+ + x_-)}{2} \text{ if both } x_+, x_- \ll 1 \quad (3)$$

$$\text{and, with } \Delta p \equiv p_+ - p_-, \; x_{\Delta p} = x_- - x_+. \quad (4)$$

We assume that the tail due to lost energy can be represented by a sum of exponentials for p_+ and p_- separately,

$$P^{\pm}(x_{\pm}) = \sum_{j=1,N} f_j^{\pm} b_j^{\pm} e^{-b_j^{\pm} x_{\pm}} \quad (5)$$

The probabilities $P^{\pm}$ are normalised to 1 so long as the tails are confined to $x_{\pm} \ll 1$. The spike at $x_{\pm} = 0$ can be reproduced by using large values of $b_1^{\pm}$. Figure 5 shows how the x variables relate to the 'LEGO' plot of p_+ versus

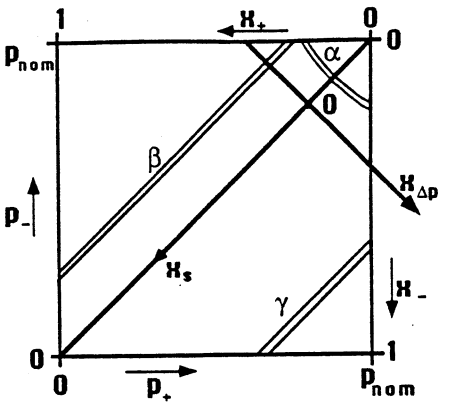

Figure 5: Conversion of momentum variables to the dimensionless x variables of equations 2, 3 and 4.

p_-, as shown in Figure 2. Convolutions of P^+ with P^- give the probability distributions for $x_{\Delta p}$ and x_s.

For $x_{\Delta p} > 0$

$$P(x_{\Delta p}) = \sum_{j,k=1,N} \frac{f_j^+ f_k^- b_j^+ b_k^-}{b_j^+ + b_k^-} e^{-b_k^- x_{\Delta p}} \tag{6}$$

i.e. integration on Figure 5 over areas like γ.

For $x_{\Delta p} < 0$

$$P(x_{\Delta p}) = \sum_{j,k=1,N} \frac{f_j^+ f_k^- b_j^+ b_k^-}{b_j^+ + b_k^-} e^{-b_j^+ x_{\Delta p}} \tag{7}$$

i.e. integration on Figure 5 over areas like β.

Note that the region of $x_{\Delta p} > 0$ is sensitive only to exponential terms from $P^-(x_-)$ and the region $x_{\Delta p} < 0$ only to terms from $P^+(x_+)$.

We also have

$$P(x_s) = 2 \sum_{j,k=1,N} \frac{f_j^+ f_k^- b_j^+ b_k^-}{b_j^+ - b_k^-} (e^{-2b_k^- x_s} - e^{-2b_j^+ x_s}) \tag{8}$$

i.e. an integration over areas like α.

After a run with a particular set of beam conditions there will be $\geq 100R$ of Bhabha events whose distributions of $\sqrt{s}$ and θ_A (equivalent to Δp) can be measured. Fits can be made to the three above equations to get $f_j^+, b_j^+, f_k^-, b_k^-$ for as many different b_j^+, b_k^- as are needed to give a good χ^2. Direct measurement of $\sqrt{s}$ will constrain the distribution directly in the part of the tail with measurably large energy losses, but the region with $x_+, x_- \leq 0.01$ will depend only on the fits to the acollinearity for almost collinear events. The well constrained b_j^+, b_k^- values from the large Bhabha statistics will give the fitted luminosity spectrum $\mathrm{d}\mathcal{L}/\mathrm{d}\sqrt{s}$ for the smaller sample of $\sim 1R$ signal events in the $t\bar{t}$ channel, for instance.

3.3.2 More realistic conditions

Realistic linac designs have a finite non-gaussian spread of beam momentum, even before beamstrahlung, but this can be measured, in principle, for both beams in their extraction-line spectrometers as mentioned above, giving distributions $P^+_{spread}(x_+)$ and $P^-_{spread}(x_-)$. These will have to be convoluted numerically with the $P^\pm(x_\pm)$ distributions introduced above (or any other suitable parametrisation). A further numerical convolution will give the predicted distributions of $\sqrt{s}$ and Δp (or θ_A) which can be compared with the observed distributions. A dirty but straightforward χ^2 minimisation will give the luminosity spectrum.

Table 3: Approximate rates for possible luminosity and signal processes

Process	Rate	Comment
Bhabha 180-300 mr.	223R	Endcap. Best statistics, adequate precision.
Bhabha 300-800 mr.	104R	Intermediate
Bhabha 800-2341 mr	8R	Barrel. Lower statistics, good precision.
$\mu^+\mu^-$	R	Low statistics, good precision.
$Z^0\gamma$	30R	Reasonable statistics. Should study further.
W^+W^-	12R	Reasonable statistics. Poor precision.
Two real γ	2R	Low statistics, reasonable precision.
$t-\bar{t}$	$\sim R$	Signal.

4 Other monitoring channels

Table 3 shows the event rates for various channels just above a supposed top-antitop threshold at 125 on 125 GeV, measured in units of R, the Q.E.D. dimuon rate. Three different regions of Bhabha scattering are shown.

As discussed, the only easily measurable quantity we have found which will be sensitive to variations of 1 part in 1000 in the colliding beam energies is acollinearity angle of final states containing two stable particles. The extra contribution from the t-channel means that the rate for Bhabha scattering far exceeds that for dimuons or for two real photons. But if we wish to unfold the luminosity spectrum with a precision of only 1 to 5 percent in $\sqrt{s}$, some of the other channels may be useful as a check. For many of them, as for Bhabha scattering, most or all of the final state particles will be completely contained and $\sqrt{s}$ can be measured directly. With a good compensating calorimeter it should be possible to measure the total energy of the W^+W^- final state to about 10 GeV. The $Z^0\gamma$ final state, with the γ unseen, is even more attractive. It has a high rate due to the resonant enhancement and the energy release of the Z decay is sufficient to throw most of the decay products clear of the obstructed forward region, even though the Z is produced with a considerable longitudinal boost. The two-jet and two-charged-lepton channels in Z decay will have different kinematic properties. The measured value of $\sqrt{s}$ for the two-charged-lepton events in $Z\gamma$ will be particularly well constrained, if it is assumed that the unseen photon is along the beam direction. This channel should be studied further.

5 Conclusions

Luminosity spectra can be monitored with sufficient precision for cross-sections to be measured, even in the region of the top-antitop threshold, so long as the linacs have reasonably low beamstrahlung, and the smallest possible momentum spread ($\simeq$ 0.15% or less). It will be necessary to monitor the extraction line beams to measure the absolute momenta and their spread. The acollinearity of Bhabha scattering is sensitive to the momentum unbalance between the interacting particles, which gives a good representation of the spread of interaction energy, and the Bhabha rate is very high compared with all interesting signal rates. The detector must measure θ to approximately 1 milliradian - not too difficult with available techniques. Other final-states may also be useful for monitoring the luminosity spectrum but none of them will have the precision, or the rate, which can be achieved with Bhabha scattering.

References

[1] M.J.Strassler and M.E.Peskin, 'Threshold production of heavy top quarks: QCD and the Higgs boson'; Phys.Rev. D43, 1500-1514(1991).

[2] OPAL collaboration, G.Alexander et al, 'Measurement of the Z^0 line shape parameters and the electroweak couplings of charged leptons'; CERN-PPE/91-67, Submitted to Z.Phys.C.

[3] J.Kent *et al*, 'Precision measurements of the SLC beam energy'; SLAC-PUB-4922, LBL-26977; presented at the IEEE particle Accelerator Conference, Chicago, March 20-23 1989.

[4] F.A.Berends *et al*: Nucl. Phys. B228, 537 (1983); and Nucl. Phys.B304 712 (1988).

[5] Pointed out by M.Mannelli, CERN, private communication.

[6] Based on the PALMER F design as represented in the BEAMSPEC program of T.Barklow, parameters provided by W.Kozanecki; see section on Collider Designs in main Top Quark Physics working group report (above).

[7] Based on the DESY-Darmstadt design in BEAMSPEC, as [6]. Beamstrahlung and beam-spread have recently been considerably reduced

when the design was reoptimised for top-threshold studies (private communication from T.Weiland).

[8] Based on the superconducting TESLA design in BEAMSPEC, as [6].